One step clustering based on a-contrario framework for detection of alterations in historical violins

Alireza Rezaei,
Sylvie Le Hégarat-Mascle,
Emanuel Aldea
SATIE Laboratory, University Paris Saclay
rue Noetzlin, Gif-sur-Yvette 91190, France
Email:firstname.lastname@universite-paris-saclay.fr

Piercarlo Dondi
Department of Electrical, Computer and Biomedical Engineering,
University of Pavia, Italy
Email: piercarlo.dondi@unipv.it

Marco Malagodi
Department of Musicology and Cultural Heritage,
University of Pavia, Italy
Email: marco.malagodi@unipv.it

***Abstract*—Preventive conservation is an important practice in Cultural Heritage. The constant monitoring of the state of conservation of an artwork helps us reduce the risk of damage and number of necessary interventions. In this work, we propose a probabilistic approach for the detection of alterations on the surface of historical violins based on an a-contrario framework. Our method is a one step NFA clustering solution which considers grey-level and spatial density information in one background model. The proposed method is robust to noise and avoids parameter tuning and any assumption about the quantity of the worn-out areas. We have used as input UV induced fluorescence (UVIFL) images for considering details not perceivable with visible light. Tests were conducted on image sequences included in the "Violins UVIFL imagery" dataset. Results illustrate the ability of the algorithm to distinguish the worn area from the surrounding regions. Comparisons with state-of-the-art clustering methods show improved overall precision and recall.**

I. Introduction

Preventive conservation, a crucial procedure in Cultural Heritage, consists in the constant monitoring of artworks and monuments to reduce the risk of damages and to minimise restorations [1], [2]. This practice is particularly complex and requires an interdisciplinary approach to correctly interpret and to manage the effects of chemical, physical and biological alterations [3], [4], [5]. Historical wood musical instruments (such as violins or violas) are a peculiar kind of artwork because they are both held in museums and played (even today), leading to a major risk of mechanical wear in the areas in direct contact with the musicians. In particular, the monitoring of historical violins presents various complexities: (i) the instruments have undergone multiple restorations during centuries, leading to a stratified surface difficult to analyse; (ii) varnish wear can evolve in different ways depending on the initial conditions of the surface and on the different substances being present; (iii) the rounded morphology and the high reflectance of the varnishes generate noisy reflections during photo acquisition (almost impossible to avoid completely) that can be confused with potential alterations; (iv) in order to avoid damages to the varnishes, violins cannot be rigidly fixed to a support, thus, slight misalignment between photographic sessions can occur. If we consider the entire surface of an instrument these last two issues are not critical; however, for detecting small alterations (especially in the initial steps) we need to focus on the areas always in contact with the musicians (mainly top left and bottom right of the back plate), taking close-up pictures of these details that are naturally more subject to this kind of acquisition noise. The combined use of multiple analytical techniques proved to be a valid approach for handling these issues [6], [7], however, mixing more techniques is a very slow and time-consuming process. A more efficient procedure will consist of regular analysis of images in order to quickly identify possible altered areas, and then apply only on them spectroscopic techniques as confirmation.

In this study, we have used multi-temporal UV induced fluorescence (UVF or UVIFL) images collected in the "Violins UVIFL imagery" dataset[1] [8]. UVIFL photography is a widely adopted non-invasive diagnostic technique that allows to see details not perceivable using visible light [9]. In particular, for the study of historical violins, UVIFL images are generally used to highlight possible restorations or interesting areas [10] and to decide where to apply more precise but slower diagnostic techniques, like X-Ray Fluorescence (XRF) [11] or Fourier Transform Infrared (FTIR) spectroscopy [12]. The possibility to see "hidden" details is particularly valuable in our scenario since it potentially allows for an early detection of new alterations. In fact, visible light can be deceptive. When a new alteration is clearly identifiable under a standard illumination, it is likely that an irreversible damage to the surface varnish has already occurred. Moreover, substances used for cleaning the instruments can temporarily hide the presence of alterations, and, thus, slow down the detection. On the contrary, the effectiveness of UVIFL photography to characterise variations in varnishes is well known in the Cultural Heritage field [13].

Then, wear detection can be viewed as a semantic segmentation problem with two semantic classes, namely the intact areas and the wear region(s). However, wear features are highly variable both in terms of radiometry and in terms of geometric shape so that we would rather cast the wear detection problem as a change detection problem assuming we have at our disposal a reference image taken from the initial state of the instrument. Then, a famous framework to handle 2-class problems with one of the class unknown (the change one) is

[1]https://vision.unipv.it/research/UVIFL-Dataset/

the a-contrario framework [14]. It takes inspiration from the statistical rejection tests with the null hypothesis ($\mathcal{H}_0$) being "the pixel does not correspond to a change". However, a-contrario approaches differ on the two following points: (i) the null hypothesis (i.e., the one to reject) is represented through a "naive" model that corresponds to unstructured data; (ii) the decision is taken based on the Number of False Alarms (or significance). In this work, we describe a new method for early detection of superficial alterations on historical violins based on the a-contrario framework [15], [16]. This method can be applied with minor modifications to any wooden instruments. Also, by replacing the acquisition and pre-processing steps, we can cover a wider variety of change detection problems. The main contribution of the proposed approach is to encompass in a single model both criteria that wear areas present: a *high density* of pixels having *different radiometry* with respect to the reference image. It also allows us to be free from any threshold decision and cluster feature specification.

II. Related works

The a-contrario framework introduced by Desolneux et al. [15] has been used in image analysis in a variety of applications such as texture analysis [17], motion detection [18], [19], edge and line detection [20], [21], [22], [23], or reconstruction from motion [24]. In all these studies, the detection is performed by rejecting a *naive model* which describes the statistic of the unstructured data. At the same time, grouping principles have been used for tasks related to the higher level perceptual organization of scenes [25], [26], thanks to their general nature.

In our case, we are interested in the applications dealing with the detection of changed areas across multi-temporal images. In early studies, the a-contrario framework and spectral invariant features have been used to detect meaningful changes between two satellite images of the same area taken at different times [27]. An a-contrario approach has also been proposed for change detection in three dimensional multi-modal medical images such as Magnetic Resonance sequences [28]. In 2010, Robin et al. use the a-contrario framework for the definition of a criterion assessing the level of coherence in a sequence of images for detecting sub-pixel changes in a time-series of satellite images [29]. Flenner et al. further investigated this approach by using exchangeable random variables instead of relying on the independent and identically distributed (IID) assumption [30]. All these works focus on the grey level values (and their changes) so that the considered naive model deal with grey level discrepancy.

Now, numerous works have been proposed to deal with objects characterized by their spatial feature consistency. Searching for a pattern using a-contrario framework can be done either by computing the significance of every pattern corresponding to a parametric shape (e.g., circle [31], line, ellipse [32]) or by checking possible clusters of points regardless of their shape [33], [34]. In these works, even if one may consider more complex models which allow for taking into account dependence in the image [35], the usual naive model that represents unstructured data is the uniform distribution, for instance of the gradient orientations in [36] or simply of the location of the 1-valued pixels in [15] and [37] that process binary images.

Based on all previous cited works, a straightforward solution considered in [22], [38] is to first use an a-contrario approach to detect points that, according to their grey level values, are likely to belong to a change area, to store these points as a binary image, and then group these points (1-valued in the binary image) together [16]. However, with such an approach the two criteria on grey level values and spatial features of the researched objects or areas are considered sequentially and there is an implicit threshold (at the end of the first step) that makes us lose the information about the intensity of the change. Our proposal is then to combine both steps and cluster a grey-level image by using a single naive model.

III. Proposed approach

A. Notations and key idea

Let $\mathcal{K} \subsetneq \mathbb{N}_+$ denote a set of indices, and let $|\mathcal{K}| = K$ denote its cardinality. A series of images I_i, $i \in \mathcal{K}$, are captured from a wood sample with pre-defined time intervals. They are in conventional RGB format. For notation convenience, in the following we assume $\mathcal{K} = \{0, \ldots, K-1\}$ so that I_0 is the original image which serves as a reference. Comparison of each I_i, $i \in \{1, \ldots, K-1\}$ with I_0 using a colour difference formula [39] gives a difference map ΔI_i. ΔI_i is a grey-level image defined on the pixel domain $\mathcal{P} \subset \mathbb{N}^2$

Our problem boils down to segmenting each image ΔI_i, $i \in \{1, \ldots, K-1\}$, with respect to semantic classes, one of which representing the wear area(s). Note that, even if, according to expert knowledge the temporal evolution of the wear areas includes some information, in the perspective of the evaluation of a new change detection algorithm, it is left aside for the wear estimation and only considered for qualitative validation of our results. Now, as already said, we will encompass both criteria characterising a wear area in ΔI_i images (radiometric and spatial) in a single naive model.

The basic idea is to extend the meaningfulness concept specifying that a cluster is all the more significant that it is very dense (i.e., its points are 'surprisingly' close) not only spatially but also in terms of grey-level differences. Now, considering grey-level differences, low values correspond (mainly) to no change and extended high values (mainly) to changes, so that a grey-level transform is required to meet the assumption that a change can be detected as surprisingly structured or dense values. Then, using the cluster NFA based on distance, the proposed method also needs the specification of the considered distance. These two points are presented in the next subsections before the NFA computation and cluster detection algorithm.

B. Grey-level transformation

Let us first enumerate the desirable properties for the researched grey-level transformation for Δ pixel values: after transformation, (i) grey level values of pixels belonging to unchanged areas shall be stretched, (ii) grey level values of

pixels belonging to change areas shall be similar and (iii) close to zero. This last property aims at controlling not only the relative values of grey-level differences but also their absolute value. Then, the grey-level function (f) that we can consider has to:

- be decreasing;
- spread no significant grey-level differences so that uniform distribution will be acceptable.

In this study, two reasonable f functions were evaluated: the inverse function and the $\tanh$ function, with satisfactory results. Both provide expected discrepancy of the grey-value cloud as shown in Fig. 1.

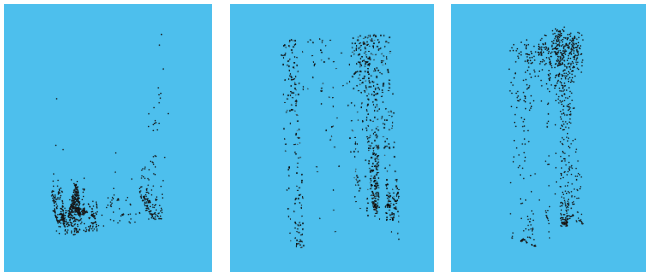

(a) (b) (c)

Fig. 1: 3D point cloud (a) before applying the function f, (b) after applying $f(x) = \frac{1}{x}$ and (c) after applying $f(x) = \tanh(th - x)$. The vertical axis represents the (transformed) grey-level values while the other two axes are for the spatial data

C. Distance between two points

The cluster detection using a-contrario is based on point distance calculation [40]. In order to take into account both spatial distance and (transformed) grey-level differences, the handled distance is a weighted sum of two terms: the 2D spatial proximity and a term representing the modified grey-level of each point. In this way, we can enforce that points with higher (f-transformed) grey-level values are considered closer together compared to points with lower grey-level. Since the grey-level values and spatial distance are inherently in different scales, we use the constant scale factor c to make them of the same order of magnitude. Note that, even if appearing as a parameter, this factor c is very easy to set based on image resolution features (spatial and radiometric). Denoting by y_i the value at pixel $i \in \mathcal{P}$, and by $D_{sp}(i,j)$ the 2D spatial distance between location of pixels i and j, $\forall (i,j) \in \mathcal{P}^2$,

$$D(i,j) = \sqrt{\left(D_{sp}(i,j)\right)^2 + c \times \left(\left(f\left(y_i\right)\right)^2 + \left(f\left(y_j\right)\right)^2\right)} \quad (1)$$

Finally, for any distance value d, a cluster $\mathcal{C} \subseteq \mathcal{P}$ is a set of points i such that $\forall i \in \mathcal{C}$, $\begin{cases} \exists j \in \mathcal{C} \text{ s.t. } D(i,j) \leq d, \\ \forall j' \in \mathcal{P} \setminus \mathcal{C}, D(i,j') > d. \end{cases}$ Note that for a given d there may be several distinct clusters $\mathcal{C}_i$ verifying previous definition. Inversely, for a given cluster $\mathcal{C}$, there is a range of distances leading to $\mathcal{C}$ that allows us to associate an inner border and an outer border to cluster $\mathcal{C}$. In the following, we denote $d_{min}(\mathcal{C})$ and $d_{max}(\mathcal{C})$ the bounds of this interval.

D. Number of False Alarms

The Number of False Alarms (NFA) is based on the considered naive model. In our case, this latter is the uniform distribution:

Definition 1 (Naive model $\mathcal{M}$)**.** *The set of points $\mathcal{S}$ is a random set of $|\mathcal{S}|$ independent uniformly distributed variables over the 3D (2D+Greylevel) space of the image.*

Note that a keypoint of a-contrario approaches is that the naive model has not to be exact, but it has only to be contradicted in the case of the researched structured data (wear in our application).

The Number of False Alarms is computed extending the NFA proposed in [16], defined for 2D cluster detection. Considering here a 3D space, the 2D surface areas are replaced by 3D volumes and the 2D distance by the distance defined in Eq. (1), so that, for any cluster $\mathcal{C}$ of 3D (2D+Greylevel) points,

$$NFA_{\mathcal{M}}(\mathcal{C}, M) = N_{test} \sum_{i=k}^{M} \binom{M}{i} \underline{V}_{\mathcal{C}}^{i} (1 - \overline{V}_{\mathcal{C}})^{M-i} \quad (2)$$

where k is the number of points in the cluster, M is the total number of points and $\underline{V}_{\mathcal{C}}$ and $\overline{V}_{\mathcal{C}}$ are the lower and upper bounds of the relative volume of the cluster compared to the whole image cube. These regions are obtained by performing morphological operations on the union of every point in the cluster [16]. In our application, for simplicity of computation, we estimate both $\underline{V}_{\mathcal{C}}$ and $\overline{V}_{\mathcal{C}}$ by utilising the area of the 2D surfaces associated with these 3D regions:

$$\begin{cases} \overline{V}_{\mathcal{C}} = \overline{A}_{\mathcal{C}} \times \max\limits_{i \in \mathcal{C}} \left(f(y_i)\right) / V_{\mathcal{P}} \\ \underline{V}_{\mathcal{C}} = \underline{A}_{\mathcal{C}} \times \max\limits_{i \in \mathcal{C}} \left(f(y_i)\right) / V_{\mathcal{P}} \end{cases} \quad (3)$$

where y_i is the grey-level of point i, f is the transformation function, $V_{\mathcal{P}}$ is the volume of the image cube, and $\overline{A}_{\mathcal{C}}$ ($\underline{A}_{\mathcal{C}}$) is the upper (lower) bound of the area of the cluster in the 2D image.

IV. Implementation

The implementation process (Figure 2) begins with an application dependent step. This step can be switched out to adapt our proposed algorithm to new applications. Once the acquisition is complete, it is imperative to make sure the two images we compare are spatially registered and have the same general lightness level. Indeed, the images can be taken in different conditions and by different operators. The algorithm should remain robust to these changes.

Next, we compute a difference map between a given frame and the reference frame (t_0). The difference map between t_0 and t_i, $i \in \{1, \ldots, K-1\}$, is created by computing the color

difference between the corresponding pixels. We have utilized the CIEDE2000 formula, after transforming the RGB values into the CIELAB color space.

It is worth noting that other approaches may also be used to create the difference map for the rest of the detection process, from a simple Euclidean distance between RGB values to more complicated color difference models. However, in our case the employed difference provides consistent results which agree with the expected wear areas.

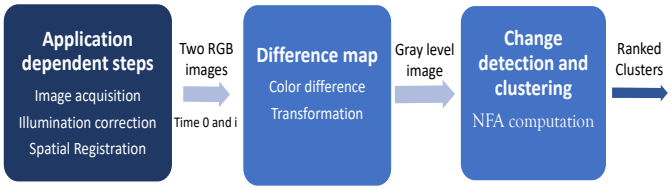

Fig. 2: General steps of the proposed algorithm

The difference image is then used for finding the clusters and computing their significance. First, we create a minimum spanning tree of the points in the difference image based on the distances computed by Eq. (1). Each sub-tree then is considered a potential cluster and by computing the meaningfulness value we decide which ones to keep and which ones to discard. Algorithm 1 describes the process step by step.

Calculating the Eq. (1) can be difficult without an approximation. In images with small pixel numbers (around 1000 or lower) we can calculate the exact values using BigInt data types. In other cases, an approximation can be viable if we restrict the area possible for a cluster compared to the whole image. Since the wear area is not covering the image, this restriction will not hinder the process.

Algorithm 1 Change detection between frame i and the reference frame

Perform the pre-processing
Compute the color difference map ΔI between I_i and I_0
for each pixel j in ΔI **do**
    $\Delta I(j) = f(\Delta I(j))$
end for
Normalize ΔI between 0 and 255
Compute the distance D_{sp} between each pair of points in ΔI
for each pair of pixels j and j' in ΔI **do**
    Compute $D(j, j')$ according to Eq. (1)
end for
Compute the minimum spanning tree T for the points in ΔI
for each subtree in T defining a cluster $\mathcal{C}$ **do**
    Compute $\underline{V_{\mathcal{C}}}$ and $\overline{V}_{\mathcal{C}}$ according to Eq. (3)
    $M \leftarrow$ the total number of points in the spanning tree
    $k \leftarrow$ the number of points in $\mathcal{C}$
    Compute NFA value (up to scale owing to N_{test}) according to Eq. (2) using values k, M, $\underline{V_{\mathcal{C}}}$ and $\overline{V}_{\mathcal{C}}$
end for
Find disjoint sub-trees with maximum NFA
Sort sub-trees according to their NFA

V. Results

A. Dataset

The "Violins UVIFL imagery" dataset is a public dataset containing multi-temporal UVIFL images of historical and sample violins. The former regularly acquired during a short period of use, the latter artificially altered in laboratory to simulate various possible alterations over a long-term use. Currently, the dataset includes image sequences of two historical violins held in Museo del Violino in Cremona (Italy), "Carlo IX" (c.1566) made by Andrea Amati and "Vesuvio" (1727) made by Antonio Stradivari, and two artificially created sample sequences. The alterations were created scrubbing the surface with a cloth damped with alcohol to reproduce, as faithfully as possible, the effect of mechanical wear during playing.

For creating the first artificial sequence, called WSO1 (Figure 3(a) and (b)), a wood sample was slowly altered several times to simulate an alteration in an area with intact varnish. This set contains one reference image of the initial state of the sample and 20 altered frames.

The second sequence, called SV01 (Figure 3(c) and (d)), contains images of the lower part of the back plate of a sample violin. This set simulates the growing of wear starting from an area already ruined and consists of one reference image and 20 altered frames.

All the images were acquired following our previously defined acquisition protocol [41], using a Nikon D4 full-frame digital camera with a 50 mm f/1.4 Nikkor objective, 30s exposure time, aperture f/8, ISO 400 and two wood lamp tubes (Philips TL-D 36 W BBL IPP low-pressure Hg tubes, 40 Watt, emission peak $\sim 365nm$) as UV-A lighting source.

For the purpose of this paper we focused only on the two artificial sequences, since the period of examination for the two historical violins was relatively short and only "Vesuvio" showed a very slight alteration on its back plate.

B. Outputs

Figure 4 shows the result of clustering for four sample frames of WS01. As we can see, small noises change from frame to frame, big artefacts have a constant size and location, and the wear area grows over time. In all cases, small noises have been ignored and significant high change areas have been identified.

C. Evaluation

For the purpose of evaluation, we need a viable existing process as an alternative for our proposal. As mentioned before, our proposal deals with a certain set of limitations and assumptions; so, it is imperative that the comparison is made with a process which can also work in those conditions. Therefore, we are looking for these features:

- Segmentation should be done using both the grey-level and the density information.

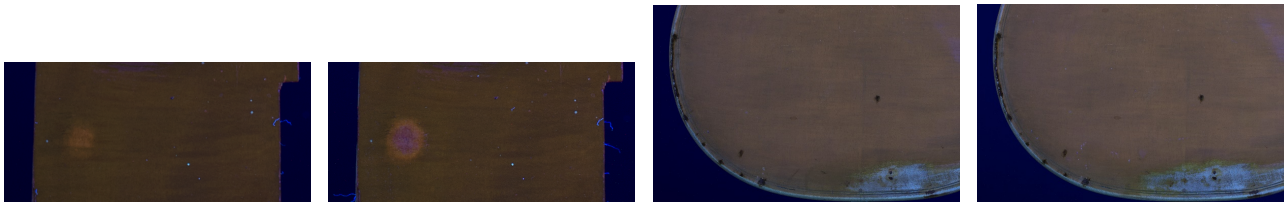

(a) (b) (c) (d)

Fig. 3: Samples UVIFL images contained in the dataset: (a) and (b) from set WS01, (c) and (d) from set SV01.

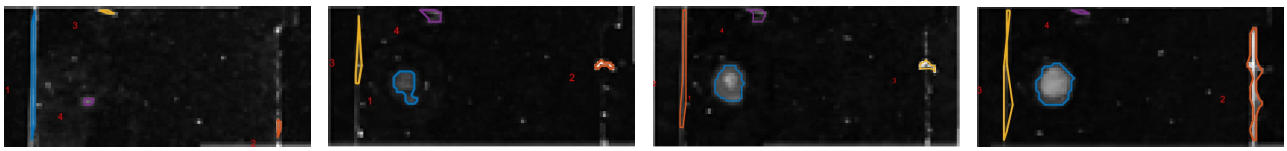

(a) (b) (c) (d)

Fig. 4: Clustering output from frames 3, 9, 15 and 20 of set WS01 using the proposed NFA clustering.

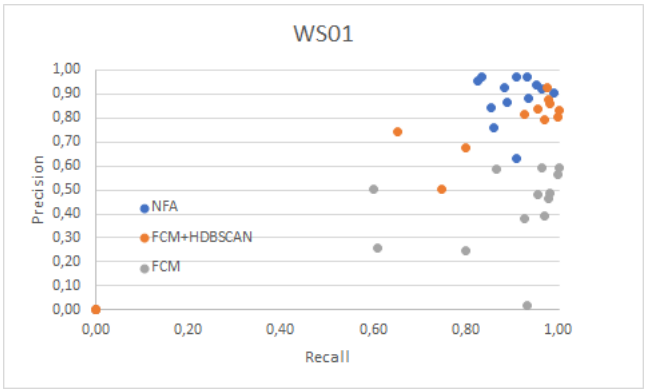

(a)

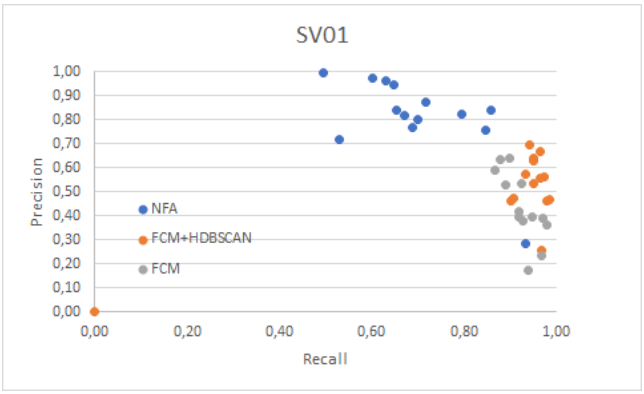

(b)

Fig. 5: Precision-Recall plot for WS01 (a) and SV01 (b). For a given algorithm (indicated by the color), each point highlights the performance at a specific timestep of the sequence.

- The available number of images in the problem domain is very limited.
- Number of clusters is unknown beforehand.
- The general shape of a wear cluster is unknown.
- There is no clear threshold between background and foreground.
- The data contains noise and artifacts.
- The process should be automatic and not interactive.
- There should be a way to rank the resulted clusters.

For separating the background from the foreground, we use FRFCM proposed by Lei et al. [42], which is a modified fuzzy cmeans algorithm. They incorporate local spatial information by using morphological reconstruction, which improves the classic fuzzy cmeans to help dealing with the different types of noise. Applying this method gives us consistently good separation between background and foreground which makes it a good candidate for the evaluation of our algorithm.

To spatially cluster the points produced from FRFCM we have chosen a density based algorithm proposed by Campello et al.[43]. HDBSCAN (or Hierarchical Density-Based Spatial Clustering, with Application with Noise) is a framework for density-based cluster analysis. The algorithm produces a complete clustering hierarchy of all possible density based clusters and - crucially for us - it also provides a global, optimal non-hierarchical solution which maximizes the overall stability of the proposed clusters. This means we can evaluate our automatic process (for the number of clusters) with a direct comparison of resulted clusters from both methods.

For the comparison to be fair, we also need to rank the produced clusters based on a specific feature. The meaningfulness value which we assign to each cluster does not directly translate to the grey-level value or shape of the cluster; but it can be mimicked generally by the area of the cluster. Therefore, we sort the results of HDBSCAN based on the number of pixels in each cluster in descending order.

The ground truth for each frame has been created manually with our best estimation as to where the wear region is. In the absence of any exact (due intrinsically to the wear construction process and to the inability to apply physico-chemical analysis

TABLE I: Comparison of the result of proposed NFA clustering, FRFCM+HDBSCAN clustering and the ground truth for examples drawn from set WS01.

No.	Ground truth	NFA clustering	FRFCM+HDBSCAN
$S_1 : 9$		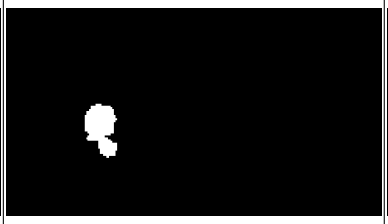	
$S_1 : 15$			
$S_1 : 20$	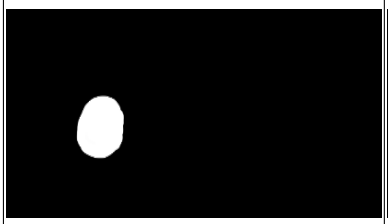	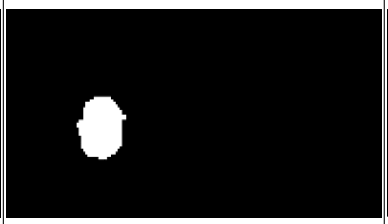	

on a large scale) knowledge on the boundaries of wear regions, they have been defined intentionally very loose.

We directly compared our $k(k \leq 4)$ most significant clusters with the first k clusters we get from the mentioned process in 4 separate comparisons. The ideal scenario is that the wear region appears as the rank 1 cluster; but depending on the position of the image in the series and on the amount of artifacts being present, we may get lower rank wear regions.

Tables I and II show three sample frames from each dataset: their ground truth and output of each method. A qualitative consideration of the results indicates:

- The proposed method has segmented the difference image with regards to both grey-level values and spatial density in one step. The background separation is done seamlessly and correctly.
- We have successfully dealt with background noise and artifacts from UV reflections in the majority of cases. For example, in dataset two, reflections on the border of the violin are very close to the actual wear region. The NFA clustering has managed to avoid them completely or to a significant degree while FRFCM+HDBSCAN have group them together with the wear in a few cases. Inherently the NFA clustering allows for controlling the number of false alarms. This results in globally better wear detection (lower false positive values by accepting more false negative values).
- The wear region has been identified without any prior assumption about its position or shape. In addition, the most significant clusters have been detected without the need for number of clusters as an input.

For quantitative evaluation, precision and recall are computed regarding three cases: our proposal, the FRFCM [42], and the combination of FRFCM[42] and HDBSCAN[43] as mentioned before.

Figure 5 shows the precision/recall charts for sequences WS01 and SVO1. For these plots the first cluster in the ranked order has been considered. In both sets, the proposed NFA clustering has better precision while maintaining an acceptable recall in most cases:

- For set WS01, in average, we achieve 87% precision and 89% recall which is higher than the average scores for FRFCM+HDBSCAN (50% precision and 75% recall). Number of failures to identify the wear region in rank one is one for NFA and three for FRFCM+HDBSCAN.
- For set SV01, which contains more noise and artifacts, on average, we achieve 77% precision and 69% recall as opposed to 46% precision and 90% recall for FRFCM+HDBSCAN. The number of failures to identify the wear region in rank one is zero for NFA and one for FRFCM+HDBSCAN.

TABLE II: Comparison of the result of proposed NFA clustering, FRFCM+HDBSCAN clustering and the ground truth for examples drawn from set SV01.

No.	Ground truth	NFA clustering	FRFCM+HDBSCAN
$S_2 : 9$	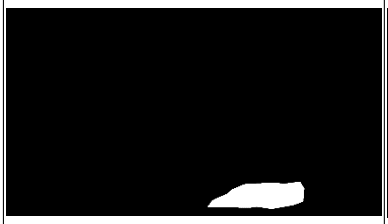		
$S_2 : 15$	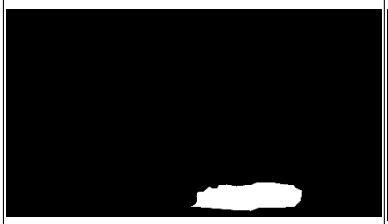		
$S_2 : 20$			

VI. Conclusion

In this paper, we introduced a probabilistic method for detecting significant changes located in clusters within a series of images. The proposed method performs an automatic clustering process directly on the grey-level difference image, while dealing with the background noise and artifacts. Comparisons with recent clustering methods show meaningful improvements while having the benefit of an inherent ranking criterion for the produced clusters.

This approach can be used in preventive conservation as a fast, preliminary examination of the surface of a violin able to identify the most likely altered areas. Thus, a verification using more precise but slower techniques (like spectroscopic analyses) will be done only on the detected areas, optimising the monitoring procedure.

For future studies, we intend to perform a long-term monitoring process considering real historical violins which are played weekly. Beside creating a valuable dataset for our community, this will allow us to validate our algorithm as well on real wear patterns.

Lastly, while in the current work we have only used one pair of images at a time to track the changes, it is interesting and useful to incorporate time information in our model. Inherently, the evolution of the wear region through time is different from that of artifacts being present in the image; this can help us differentiate wear regions better. Also, in an ongoing monitoring process it can help us detect a newly created wear at an earlier stage.

References

[1] S. Bradley, "Preventive conservation research and practice at the british museum," *Journal of the American Institute for Conservation*, vol. 44, no. 3, pp. 159–173, 2005.

[2] E. Lucchi, "Review of preventive conservation in museum buildings," *Journal of Cultural Heritage*, vol. 29, pp. 180 – 193, 2018.

[3] N. Ghedini, I. Ozga, A. Bonazza, M. Dilillo, H. Cachier, and C. Sabbioni, "Atmospheric aerosol monitoring as a strategy for the preventive conservation of urban monumental heritage: The florence baptistery," *Atmospheric Environment*, vol. 45, no. 33, pp. 5979 – 5987, 2011.

[4] R. Ortiz and P. Ortiz, "Vulnerability index: A new approach for preventive conservation of monuments," *International Journal of Architectural Heritage*, vol. 10, no. 8, pp. 1078–1100, 2016.

[5] A. Perles, E. Pérez-Marín, R. Mercado, J. D. Segrelles, I. Blanquer, M. Zarzo, and F. J. Garcia-Diego, "An energy-efficient internet of things (IoT) architecture for preventive conservation of cultural heritage," *Future Generation Computer Systems*, vol. 81, pp. 566 – 581, 2018.

[6] G. V. Fichera, M. Albano, G. Fiocco, C. Invernizzi, M. Licchelli, M. Malagodi, and T. Rovetta, "Innovative monitoring plan for the preventive conservation of historical musical instruments," *Studies in Conservation*, vol. 63, no. sup1, pp. 351–354, 2018.

[7] T. Rovetta, C. Invernizzi, G. Fiocco, M. Albano, M. Licchelli, M. Gulmini, G. Alf, D. Fabbri, A. Rombolà, and M. Malagodi, "The case of antonio stradivari 1718 ex-san lorenzo violin: History, restorations and conservation perspectives," *Journal of Archaeological Science: Reports*, vol. 23, pp. 443–450, 2019.

[8] P. Dondi, L. Lombardi, M. Malagodi, and M. Licchelli, "Segmentation of multi-temporal uv-induced fluorescence images of historical violins," in *New Trends in Image Analysis and Processing – ICIAP 2019*, ser. Lecture Notes in Computer Science, vol. 11808. Springer International Publishing, 2019, pp. 81–91.

[9] K. Janssens and R. Van Grieken, *Non-destructive micro analysis of cultural heritage materials*. Elsevier, 2004, vol. 42.

[10] P. Dondi, L. Lombardi, C. Invernizzi, T. Rovetta, M. Malagodi, and M. Licchelli, "Automatic analysis of uv-induced fluorescence imagery of historical violins," *J. Comput. Cult. Herit.*, vol. 10, no. 2, pp. 12:1–12:13, 2017.

[11] T. Rovetta, C. Invernizzi, M. Licchelli, F. Cacciatori, and M. Malagodi, "The elemental composition of stradivari's musical instruments: new results through non-invasive edxrf analysis," *X-Ray Spectrometry*, vol. 47, no. 2, pp. 159–170, 2018.

[12] C. Invernizzi, G. V. Fichera, M. Licchelli, and M. Malagodi, "A non-invasive stratigraphic study by reflection ft-ir spectroscopy and uv-induced fluorescence technique: The case of historical violins," *Microchemical Journal*, vol. 138, pp. 273 – 281, 2018.

[13] M. Thoury, M. Elias, J. M. Frigerio, and C. Barthou, "Nondestructive varnish identification by ultraviolet fluorescence spectroscopy," *Appl. Spectrosc.*, vol. 61, no. 12, pp. 1275–1282, Dec 2007.

[14] A. Desolneux, L. Moisan, and J.-M. Morel, "Gestalt theory and computer vision," in *Seeing, Thinking and Knowing*. Springer, 2004, pp. 71–101.

[15] ——, "Meaningful alignments," *International journal of computer vision*, vol. 40, no. 1, pp. 7–23, 2000.

[16] A. Desolneux, L. Moisan, and J.-M. More, "A grouping principle and four applications," *IEEE Transactions on Pattern Analysis and Machine Intelligence*, vol. 25, no. 4, pp. 508–513, 2003.

[17] B. Grosjean and L. Moisan, "A-contrario detectability of spots in textured backgrounds," *Journal of Mathematical Imaging and Vision*, vol. 33, no. 3, p. 313, 2009.

[18] T. Veit, F. Cao, and P. Bouthemy, "An a contrario decision framework for region-based motion detection," *International journal of computer vision*, vol. 68, no. 2, pp. 163–178, 2006.

[19] ——, "Space-time a contrario clustering for detecting coherent motions," in *Proceedings 2007 IEEE International Conference on Robotics and Automation*. IEEE, 2007, pp. 33–39.

[20] N. Widynski and M. Mignotte, "A contrario edge detection with edgelets," in *2011 IEEE International Conference on Signal and Image Processing Applications (ICSIPA)*. IEEE, 2011, pp. 421–426.

[21] C. Akinlar and C. Topal, "Edlines: A real-time line segment detector with a false detection control," *Pattern Recognition Letters*, vol. 32, no. 13, pp. 1633 – 1642, 2011.

[22] E. Aldea and S. Le Hégarat-Mascle, "Robust crack detection for unmanned aerial vehicles inspection in an a-contrario decision framework," *Journal of Electronic Imaging*, vol. 24, no. 6, pp. 061 119–061 119, 2015.

[23] G. Liu, Y. Gousseau, and F. Tupin, "A contrario comparison of local descriptors for change detection in very high spatial resolution satellite images of urban areas," *IEEE Transactions on Geoscience and Remote Sensing*, 2019.

[24] P. Moulon, P. Monasse, and R. Marlet, "Adaptive structure from motion with a contrario model estimation," in *Asian Conference on Computer Vision*. Springer, 2012, pp. 257–270.

[25] E. Michaelsen, "Self-organizing maps and gestalt organization as components of an advanced system for remotely sensed data: An example with thermal hyper-spectra," *Pattern Recognition Letters*, vol. 83, pp. 169 – 177, 2016, advances in Pattern Recognition in Remote Sensing.

[26] Y. Yan, J. Ren, G. Sun, H. Zhao, J. Han, X. Li, S. Marshall, and J. Zhan, "Unsupervised image saliency detection with gestalt-laws guided optimization and visual attention based refinement," *Pattern Recognition*, vol. 79, pp. 65 – 78, 2018.

[27] J. L. Lisani and J.-M. Morel, "Detection of major changes in satellite images," in *Proceedings 2003 International Conference on Image Processing (Cat. No. 03CH37429)*, vol. 1. IEEE, 2003, pp. I–941.

[28] F. Rousseau, S. Faisan, F. Heitz, J.-P. Armspach, Y. Chevalier, F. Blanc, J. de Seze, and L. Rumbach, "An a contrario approach for change detection in 3d multimodal images: application to multiple sclerosis in mri," in *2007 29th Annual International Conference of the IEEE Engineering in Medicine and Biology Society*. IEEE, 2007, pp. 2069–2072.

[29] A. Robin, L. Moisan, and S. Le Hégarat-Mascle, "An a-contrario approach for subpixel change detection in satellite imagery," *IEEE TPAMI*, vol. 32, no. 11, pp. 1977–1993, 2010.

[30] A. Flenner and G. Hewer, "A helmholtz principle approach to parameter free change detection and coherent motion using exchangeable random variables," *SIAM Journal on Imaging Sciences*, vol. 4, no. 1, pp. 243–276, 2011.

[31] C. Akinlar and C. Topal, "Edcircles: A real-time circle detector with a false detection control," *Pattern Recognition*, vol. 46, no. 3, pp. 725–740, 2013.

[32] V. Pătrăucean, P. Gurdjos, and R. G. von Gioi, "Joint a contrario ellipse and line detection," *IEEE TPAMI*, vol. 39, no. 4, pp. 788–802, 2017.

[33] G. Palma, I. Bloch, and S. Muller, "Detection of masses and architectural distortions in digital breast tomosynthesis images using fuzzy and a contrario approaches," *Pattern Recognition*, vol. 47, no. 7, pp. 2467–2480, 2014.

[34] S. Zair, S. Le Hégarat-Mascle, and E. Seignez, "A-contrario modeling for robust localization using raw GNSS data," *IEEE Transactions on Intelligent Transportation Systems*, vol. 17, no. 5, pp. 1354–1367, 2016.

[35] A. Myaskouvskey, Y. Gousseau, and M. Lindenbaum, "Beyond independence: An extension of the a contrario decision procedure," *International journal of computer vision*, vol. 101, no. 1, pp. 22–44, 2013.

[36] R. G. Von Gioi, J. Jakubowicz, J.-M. Morel, and G. Randall, "Lsd: A fast line segment detector with a false detection control," *IEEE transactions on pattern analysis and machine intelligence*, vol. 32, no. 4, pp. 722–732, 2008.

[37] S. Le Hégarat-Mascle, E. Aldea, and J. Vandoni, "Efficient evaluation of the number of false alarm criterion," *EURASIP Journal on Image and Video Processing*, vol. 2019, no. 1, p. 35, Feb 2019.

[38] A. Rezaei, E. Aldea, P. Dondi, M. Malagodi, and S. Le Hégarat-Mascle, "Detecting alterations in historical violins with optical monitoring," in *Proceedings of the 14th International Conference on Quality Control by Artificial Vision (QCAV)*, vol. 11172, 2019. [Online]. Available: https://doi.org/10.1117/12.2521702

[39] M. R. Luo, G. Cui, and B. Rigg, "The development of the cie 2000 colour-difference formula: Ciede2000," *Color Research & Application: Endorsed by Inter-Society Color Council, The Colour Group (Great Britain), Canadian Society for Color, Color Science Association of Japan, Dutch Society for the Study of Color, The Swedish Colour Centre Foundation, Colour Society of Australia, Centre Français de la Couleur*, vol. 26, no. 5, pp. 340–350, 2001.

[40] A. Desolneux, L. Moisan, and J.-M. Morel, *From gestalt theory to image analysis: a probabilistic approach*. Springer Science & Business Media, 2007, vol. 34.

[41] P. Dondi, L. Lombardi, M. Malagodi, M. Licchelli, T. Rovetta, and C. Invernizzi, "An interactive tool for speed up the analysis of UV images of Stradivari violins," in *New Trends in Image Analysis and Processing - ICIAP 2015 Workshops*, ser. Lecture Notes in Computer Science, vol. 9281. Springer International Publishing, September 2015, pp. 103–110.

[42] T. Lei, X. Jia, Y. Zhang, L. He, H. Meng, and A. K. Nandi, "Significantly fast and robust fuzzy c-means clustering algorithm based on morphological reconstruction and membership filtering," *IEEE Transactions on Fuzzy Systems*, vol. 26, no. 5, pp. 3027–3041, 2018.

[43] R. J. Campello, D. Moulavi, A. Zimek, and J. Sander, "Hierarchical density estimates for data clustering, visualization, and outlier detection," *ACM Transactions on Knowledge Discovery from Data (TKDD)*, vol. 10, no. 1, pp. 1–51, 2015.